CHAPTER 6

Gold anticancer metallodrugs: Computational strategies to identify potential candidates

IN THIS CHAPTER-

- INTRODUCTION
- METHODOLOGY
- QSAR MODELING
- MOLECULAR DOCKING
- ADME TOXICITY STUDY

OUTLOOK-

- ✓ We have investigated some selected gold (III) complexes using DFT.
- ✓ DFT study reveals that compound 1 and 3 are found to be the most stable and compound 5 is found to be the most unstable one.
- ✓ DFT based regression models reveal that DFT based descriptors are certainly play a role on the cytotoxicity of such biologically active systems.
- ✓ Molecular docking study confirms that the selected gold complexes are effective inhibitor of the target protein *h*TrxR.
- ✓ The pharmacokinetics property of the complexes are also evaluated using ADME toxicity study.
- ✓ .Based on regression, molecular docking along with ADME toxicity studies, we can conclude that ethylenediamine, cyclam and meso-tetraarylporphyrins ligand containing compounds are the best molecules in terms of stability, safety and efficacy.

6.1 Introduction

In the past few decade, Gold (III) complexes have been recognized for their encouraging anticancer activity.[1-3] Indeed, some of the gold complexes such as gold (III) porphyrins[4], dithiocarbamates[5] and polyamines[6] are also found to be chemically suitable for pharmacological study and produce cytotoxic effect on cancerous cell lines both *in vitro* as well as *in vivo*.[7,8] Apart form this there are also some bipyridyl motif containing gold (III) complexes showing marked activity against a varity of human caner cell lines.[9] Thus, the study of gold (III) complexes endowed high anticancer activity are of current interest.[10,11]

The idea of using a metallo drug as an anticancer agent came way back in 1965 with the serendipitous discovery of platinum anticancer agent *cis*-DDP.[12,13] Despite being used for over seventy years for the advancement of the symptoms associated with rheumatoid arthritis, the recognization of the anticaner potential of this class of gold complexes is a relatively recent phenomenon.[2] The basic reason for proffering its anticancer potential is the fact that it resembles Pt (II); both are having same outer electronic configuration ($5d^8$), having square planner coordination geometry.[14,15]

However, in comparison to Pt (II) complexes, Au (III) complexes are very much photosensitive and easily reduced to metallic gold.[2] But during late 90's, there was a revival of interest towards Au (III) based anticancer drugs derived from some novel compounds, endowed with improved stability and enhancing pharmacological activity.[16] In order to increase the overall stability of Au (III) complexes, multidentate ligands such as polyamide, cyclam, terpyridine and phenathroline are coordinated.[17] It has been found that these complexes are quite stable which opening the way of extensive pharmacological testing *in vitro*.[18]

Earlier reports are available where the *in vitro* assessment of the complexes have been performed by sulforhodamine B assay on the representative human ovarian tumour cell line A2780 and cisplatin resistance cell lines.[15] In most cases, the investigated compounds show relevant *in vitro* anticancer properties with IC_{50} values generally falling in the low μM range. Maria Pia Rigobello et al.[19] first reported that gold complexes can affect the mitochondrial respiratory chain and thus, cell death is induced through mitochondrial inhibition.[20]

Initially, mitochondria are solely considered as cellular energy powerhouse, but at present, it is also believed to play an essential role in apoptosis and programmed cell death.[17,21] It has been well established that gold complexes, at submolecular concentration, induces mitochondrial swelling, decreases the membrane potential.[22-24] It also inhibits mitochondrial thioredoxin reductase activity, with the IC_{50} in the range 0.020-1.42μM, which again in turn influences the membrane permeability conditions or act directly on the membrane potential, ultimately leads to cell death.[18,25]

In this chapter, we have investigated some selected gold (III) complexes (Figure 6.1) using DFT. DFT has been used extensively to predict the biological activity/toxicity/property as well as for site selectivity for the pharmaceutically active molecules. The basic objective here is to develop some effective QSAR model in order to predict the biological activity, perform the molecular docking calculations to ensure their binding ability with target proteins and finally, to carry out the ADME toxicity study to ensure the complex viability.

6.2 Methodology

6.2.1 QSAR Modelling

We calculated all the DFT based reactivity parameters using $DMol^3$ programme.[26] The compounds are subjected to full geometry optimization using double numerical with polarization (DNP) basis set in combination with the hybrid BLYP functional.[27,28] The DNP basis set is comparable to Gaussian 6-31G** basis set.[29,30] However, it is found to be much more accurate than Gaussian basis set of the same size. The physiochemical parameters namely hydration energy (HE), logP, surface area (SA), molar refractivity (MR) and polarizability (Pol) are computed using Hyperchem software for all compounds.[31] These parameters are used to generate some QSAR models in order to correlate with the cytotoxicity (pIC_{50}) of the studied compounds.

6.2.2 Molecular Docking Simulation

Molecular docking studies have been carried out in order to ensure the feasible binding site and binding affinity of the selected Au-complexes with their target protein. We have employed Molegro Virtual Docker (MVD) 5.0 (Molegro ApS, Aarhus, Denmark) for our docking simulation.[32] The basic idea of this docking stimulation is to characterize the binding site, study the orientation of the complex

with respect to the binding cavity and evaluation of strength of the interaction.[33] Since, the cellular target, thioredoxin reductase[34] (*h*TrxR, PDB id: 3QFA), of these complexes is already reported, we have done the docking simulation to retrieve information from the system. In order to locate the active potential interacting site, the cavity detection algorithm in MVD is used. We have not taken into account the water molecules in our study.[32] A set of 50 runs are given for each docking study using 2000 interactions and both the Rerank score and MolDock score are evaluated. The best fit score was obtained on the basis of the Rerank score.

6.2.3 Absorption Distribution Metabolism Excretion-Toxicity (ADME-TOX)

The pharmacokinetic properties of a molecule are carried out by the ADMET study where absorption, distribution, metabolism, excretion and toxicity of the compound is investigated.[35] In absorption, the movement of a drug into the body from the site of administration is studied because the systematic circulation of a drug is highly depends upon absorption. Distribution is the movement of the drug from intravascular to extravascular compartment. Once the drug enters into the site of its action, the metabolism of the drug occurs for its better efficacy by chemical transformation. The extra dose of a drug that is given to a patient is necessary to eliminate so as to avoid toxicity from the drug or metabolite accumulation.[36]

In our study, we have considered all the selected gold complexes for the assessment of ADMET properties. The ADME toxicity for all compound are evaluated using pkCSM online tool.[36] The pkCSM is developed on graph-based signatures method which can effectively describe the ADMET properties of drug molecules. The tool is a freely accessible web server which provides an integrated platform to evaluate pharmacokinetic and toxicity properties.

6.3 Results and Discussion

6.3.1 Structural Profile and Evaluation of Descriptors

The optimized structure obtained from BLYP/DNP level calculation for the various substituted gold (III) complexes are shown in Figure 6.2. Based on these calculations, different descriptors such as the energy of highest occupied molecular orbital (E_{HOMO}), energy of the lowest unoccupied molecular orbital (E_{LUMO}), energy difference between LUMO and HOMO ($E_{L\text{-}H}$), electorphilicity (ω), hardness (η) etc along with the physico-chemical descriptors *viz*, SA, MR and polarizability are also

selectively evaluated. The values of calculated descriptors are presented in Table 6.1, along with their pIC_{50} values. The HOMO and LUMO descriptors are frequently used as these orbitals can influence the chemical reactivity and hence their activity.[37]

Special attention has been paid on the energy difference between the LUMO and HOMO (E_{L-H}), electorphilicity (ω), hardness (η) and chemical potential (μ) in order to check the stability and reactivity of the studied complexes.

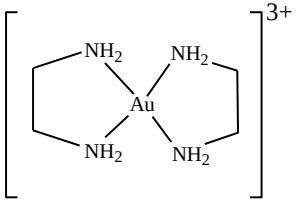

Compound 1: $[Au(en_2)]^{3+}$

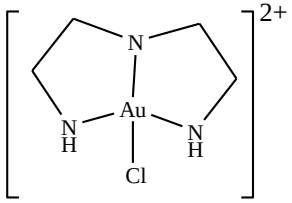

Compound2:$[Au(dien)Cl]^{2+}$

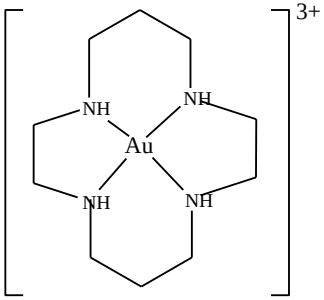

Compound3: $[Au(cyclam)]^{3+}$

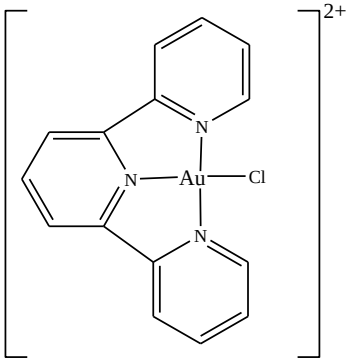

Compound4:$[Au(terpy)Cl]^{2+}$

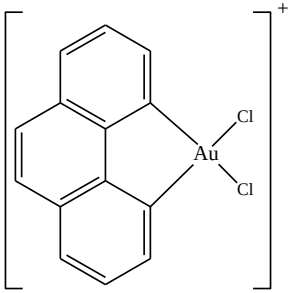

Compound5:$[Au(phen)Cl_2]^{+}$

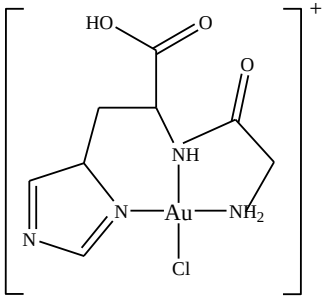

Compound 6: Chloro-glycylhistidinate Au (III) GHAu

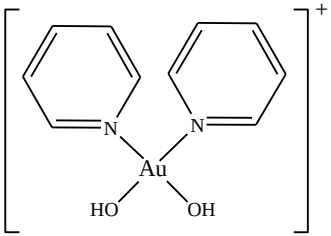

Compound 7: $[Au(bipy)(OH)_2]^{+}$

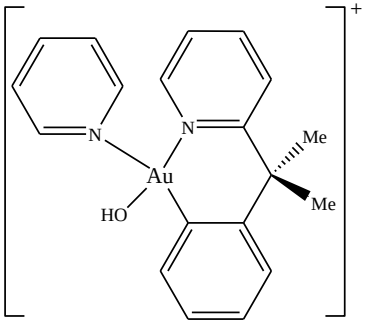

Compound8: $[Au(bipy^{c}\text{-}H)(OH)]^{+}$

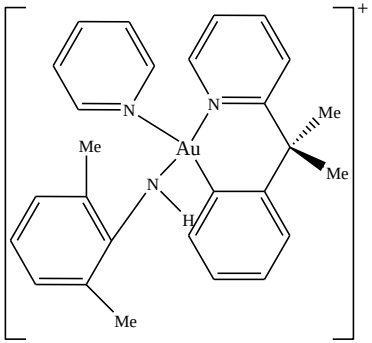

Compound9: $[Au(bipy^{dmb}\text{-}H)(2,6\text{-xylidine-}H)]^{+}$ $bipy^{dmb}$=6-(1,1-dimethylbenzyl)-2,2/-bipyridine

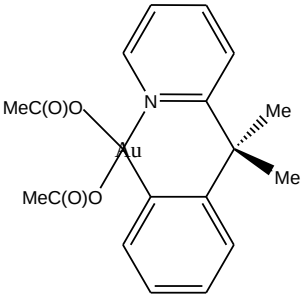

Compound10: $[Au(py^{dmb}\text{-}H)(AcO)_2]$ py^{dmb}=2-(1,1-dimethylbenzyl)-pyridine

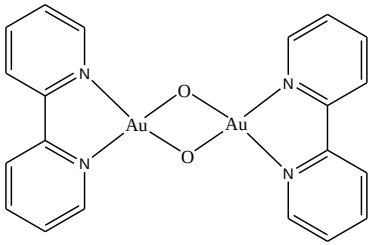

Compound11: $[Au_2(N,N)_2(\mu\text{-}O)_2]$ N,N=2,2′-bipyridine

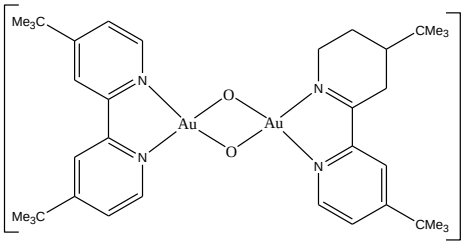

Compound12: $[Au_2(N,N)_2(\mu\text{-}O)_2]$ N,N=4,4′-di-tertbutyl

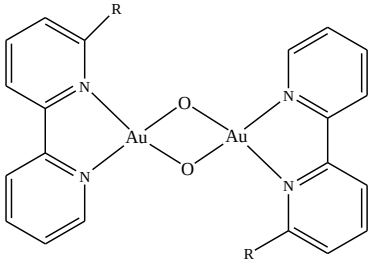

Componud 13-15: $[Au_2(N,N)_2(\mu\text{-}O)_2]$

Compound	R
Compound13	Me
Compound 14	CH_2Me_3
Compound 15	$C_6H_3Me_2$-2,6

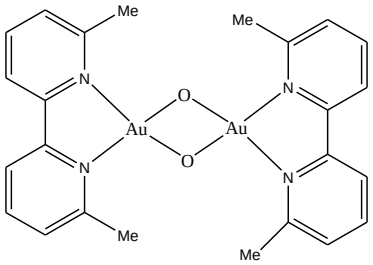

Compound16: $[Au_2(N,N)_2(\mu\text{-}O)_2]$N,N=6,6′-dimethyl-2,2′-bipyridine

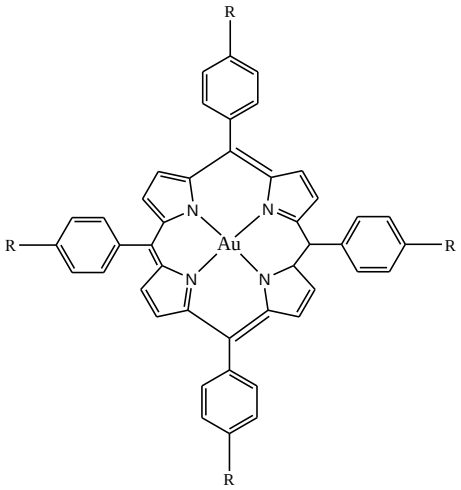

Componud17-21: [Au(III)(p-Y-TPP)]

Compound	R
Compound17	H
Compound 18	Me
Compound 19	OMe
Compound 20	Br
Compound 21	Cl

Figure 6.1 Sketch of the investigated Au (III) complexes

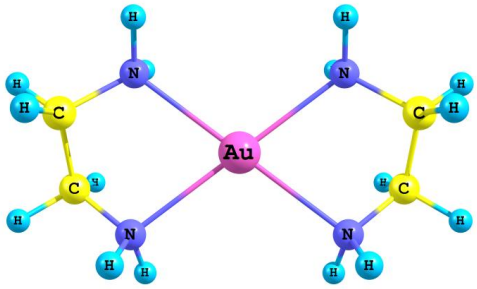

Compound 1

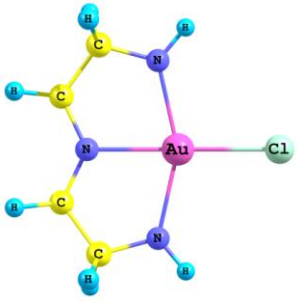

Compound 2

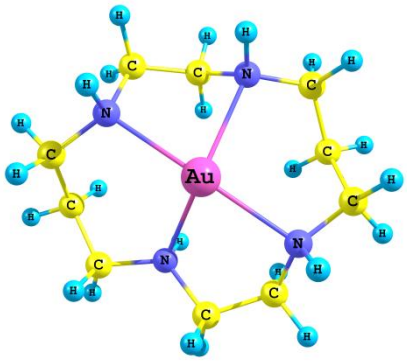

Compound 3

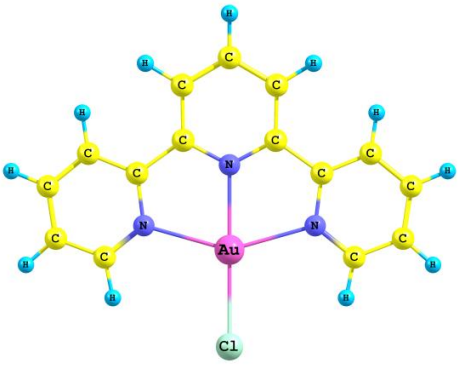

Compound 4

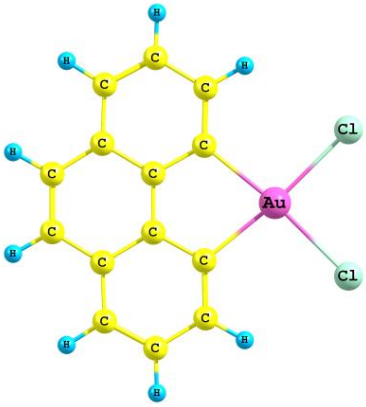

Compound 5

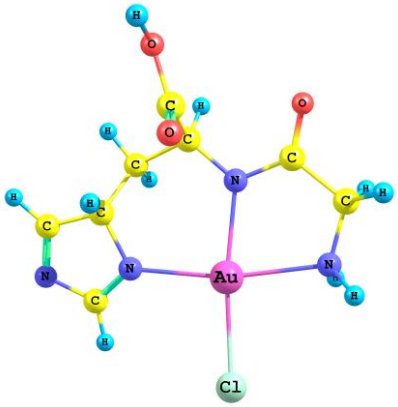

Compound 6

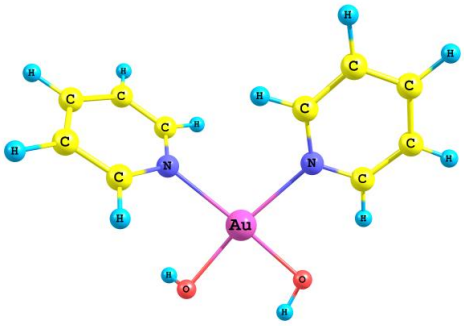

Compound 7

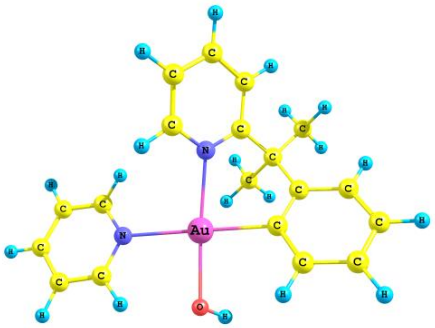

Compound 8

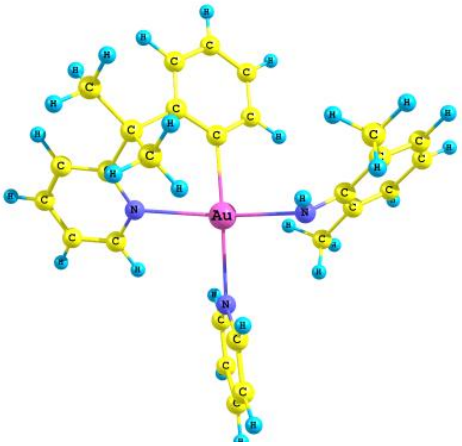

Compound 9

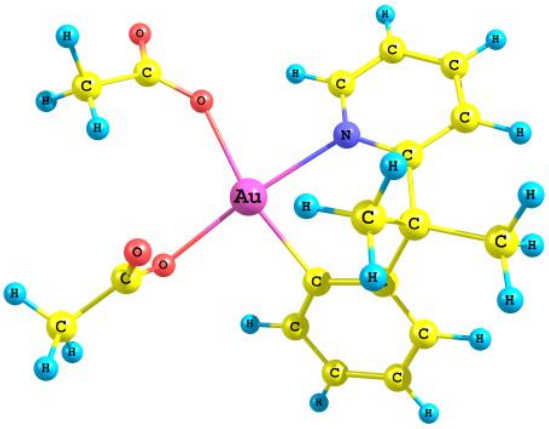

Compound 10

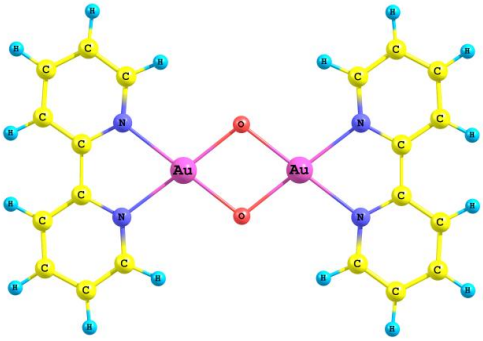

Compound 11

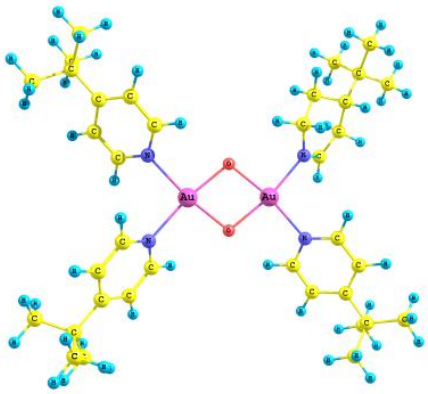

Compound 12

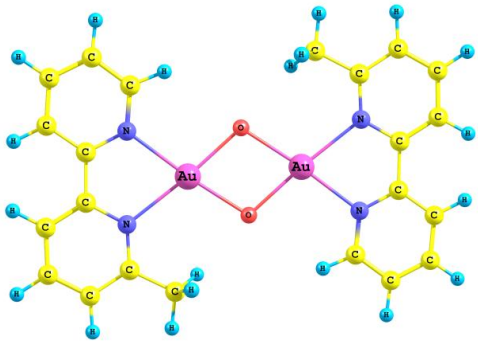

Compound 13

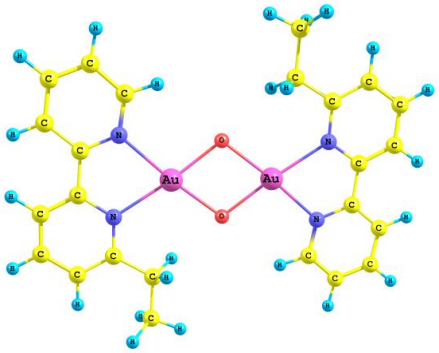

Compound 14

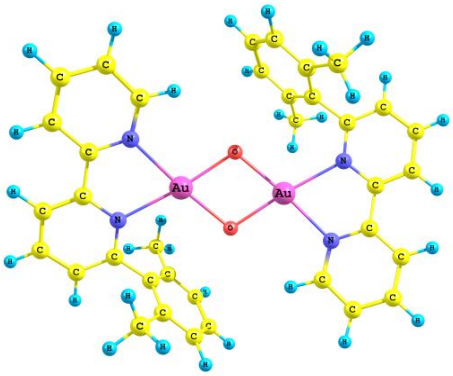

Compound 15

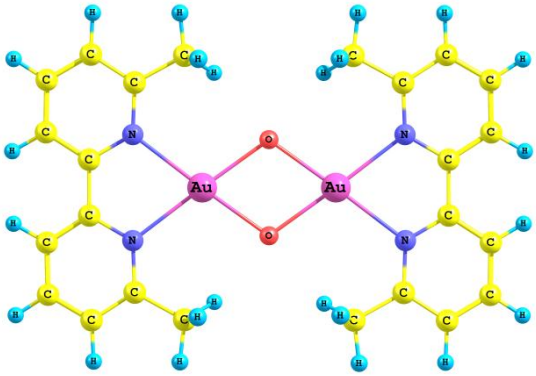

Compound 16

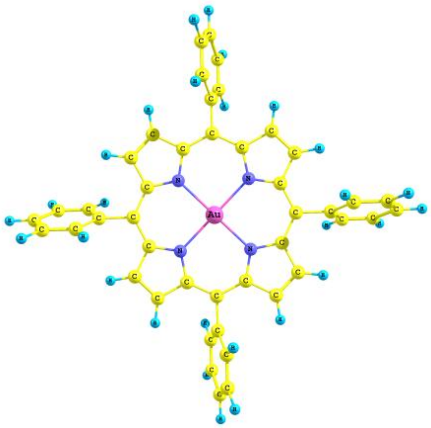

Compound 17

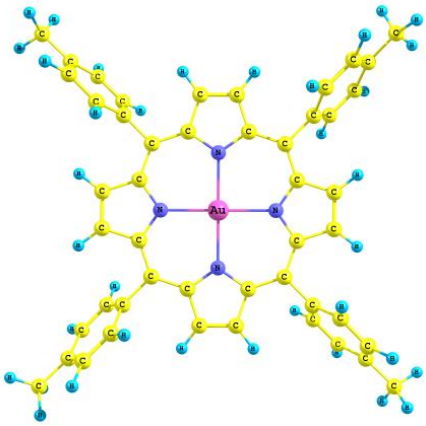

Compound 18

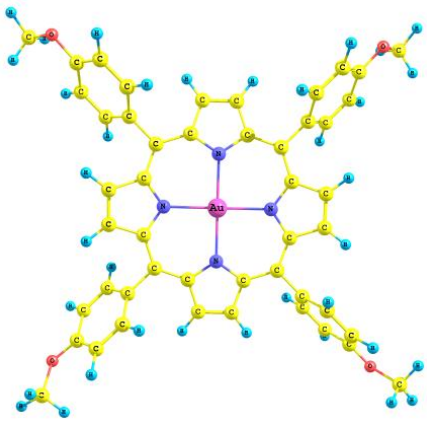

Compound 19

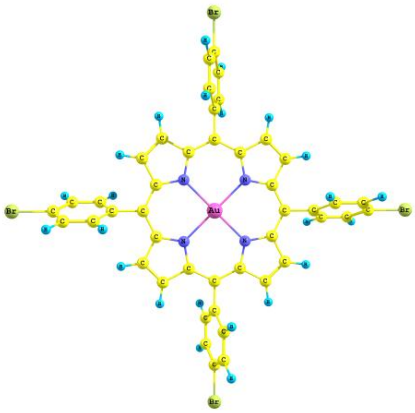

Compound 20

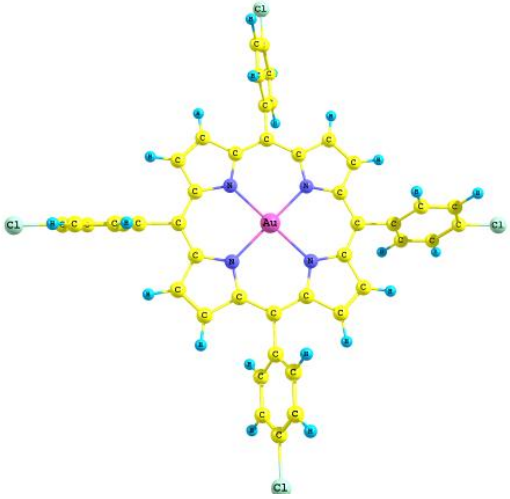

Compound 21

Figure 6.2 Optimized geometries of Au (III) complexes with levelling of the elements obtained from BLYP/DNP calculation

Table 6.1 Calculated values of all the selected descriptors for all compounds in gas phase

No.	E_{HOMO}	E_{LUMO}	E_{NL}	$E_{(HOMO-1)}$	E_{L-H}	η/au	μ/au	ω/au	SA	HE	logP	MR	Pol	R_j^2	pIC_{50}
1	-0.16	-0.148	-0.098	-0.197	0.012	0.006	-0.154	1.976	341.49	-11.79	-3.28	25.25	11.18	0.705	8.36±.77
2	-0.612	-0.599	-0.466	-0.638	0.013	0.007	-0.606	28.202	338.9	-7.68	-0.18	34.09	14.06	0.678	8.2±.93
3	-0.549	-0.527	-0.524	-0.55	0.023	0.011	-0.538	13.157	340.83	-0.1	-2.55	50.63	20.64	0.645	9.9±1.1
4	-0.467	-0.457	-0.384	-0.489	0.01	0.005	-0.462	21.344	403.31	-5.47	0.21	86.91	30.86	0.722	0.2
5	-0.368	-0.364	-0.284	-0.369	0.004	0.002	-0.366	33.489	371.69	-2.09	3.34	19.42	27.4	0.783	3.8±1.1
6	-0.338	-0.328	-0.26	-0.363	0.01	0.005	-0.333	11.089	387.88	-12.64	-1.73	53.37	21.83	0.764	5.2±1.63
7	-0.32	-0.304	-0.225	-0.354	0.015	0.008	-0.312	6.084	426.92	-23.13	-0.52	59.5	22.36	0.69	8.8±3.9
8	-0.27	-0.257	-0.204	-0.329	0.014	0.007	-0.264	5.341	486.95	-11.08	0.34	99.68	36.11	0.689	3.3±1.4
9	-0.251	-0.237	-0.184	-0.269	0.014	0.007	-0.244	4.253	611.39	-5.08	1.2	139.26	50.16	0.713	2.5±.43
10	-0.673	-0.658	-0.504	-0.715	0.015	0.008	-0.666	29.526	545.57	-5.61	0.49	93.36	34.89	0.647	2.9±.34
11	-0.394	-0.377	-0.375	-0.414	0.017	0.009	-0.386	8.742	548.56	-16.96	2.66	109.19	40.35	0.726	22.8±1.53
12	-0.368	-0.351	-0.346	-0.389	0.017	0.009	-0.36	7.602	1215.57	-3.61	5.73	182.66	71.64	0.691	12.1±1.5
13	-0.394	-0.376	-0.37	-0.412	0.018	0.009	-0.385	8.235	586.98	-11.41	2.72	120.77	44.02	0.704	25.4±2.47
14	-0.391	-0.373	-0.368	-0.41	0.018	0.009	-0.382	8.107	640.56	-9.35	3.65	129.82	47.69	0.74	12.7±1.06
15	-0.364	-0.344	-0.341	-0.377	0.02	0.01	-0.354	6.266	700.25	-6.25	4.67	185.9	67.01	0.732	11±1.5
16	-0.395	-0.374	-0.365	-0.409	0.021	0.011	-0.385	7.04	662.66	-7.14	3.7	131.03	47.69	0.703	1.79±.17
17	-0.256	-0.245	-0.221	-0.284	0.011	0.006	-0.251	5.705	638.68	-7.84	9.15	35.03	74.92	0.778	0.73±.02
18	-0.248	-0.237	-0.213	-0.275	0.011	0.006	-0.243	5.346	824.94	-3.16	10.41	53.46	82.26	0.641	1.53±.03
19	-0.235	-0.225	-0.202	-0.258	0.01	0.005	-0.23	5.29	896.05	-14.69	8.18	60.72	84.81	0.771	0.88±.02
20	-0.259	-0.248	-0.224	-0.286	0.011	0.006	-0.254	5.842	832.84	-6.52	12.76	64.28	85.43	0.748	1.12±.09
21	-0.261	-0.25	-0.226	-0.288	0.011	0.006	-0.256	5.935	794.89	-6.56	11.66	53.01	82.64	0.701	0.87.03

6.3.2 Stability and Reactivity Index

We have investigated stability and reactivity of the selected complexes using DFT based parameters. DFT has been extensively used for describing reactivity and site selectivity of numerous bioactive molecules.[38,39] The prime objectives for these reactivity descriptors are essentially to quantify and analyze the conceptually important quantities such as chemical reactivity, selectivity and stability of the molecular systems from a general theoretical framework. There have been numerous works in this field bringing out the usefulness of these descriptors in generalizing the chemical reactivity problems within the framework of DFT.[40]

The stability of any system can be explained with the help of the difference between the frontier orbitals *i.e.* the (E_{L-H}). Recent investigations revealed that this energy gap between the frontier orbitals is one of the important stability index. The most stable electronic structure has the largest HOMO–LUMO energy gap.[41] The energy gap between the frontier orbitals for all the complexes are depicted in Figure 6.3. From this Figure, it has been found that complex 3 have the most stable structure, having highest HOMO-LUMO gap and complex 5 is found to be most unstable.

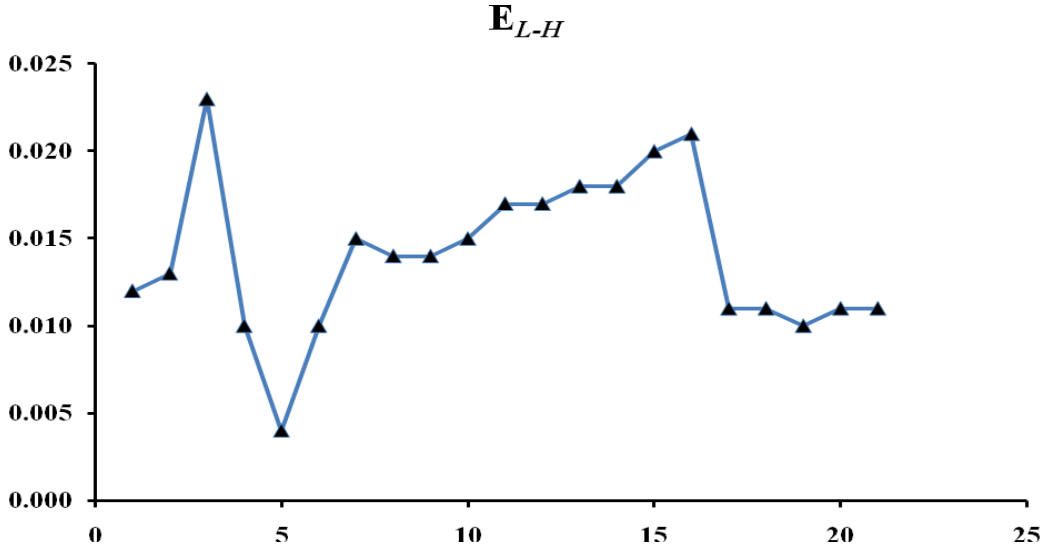

Figure 6.3 Variation of the energy gap of the frontier orbitals of the complexes

We have also implicated the MHP (maximum hardness principle)[42] and MEP (minimum electrophilicity principle)[43] in order to confirm the stability and reactivity order of the studied complexes. The MHP and MEP principles are among the most

widely accepted electronic structure principles of chemical reactivity and stability. The MHP affirms that, at a given temperature, molecular systems evolve to a state of maximum hardness. The variation of chemical hardness for all the complexes is shown in Figure 6.4. From this figure also it has been found that complex 3 have the most stable structure whereas complex 5 is the most unstable one.

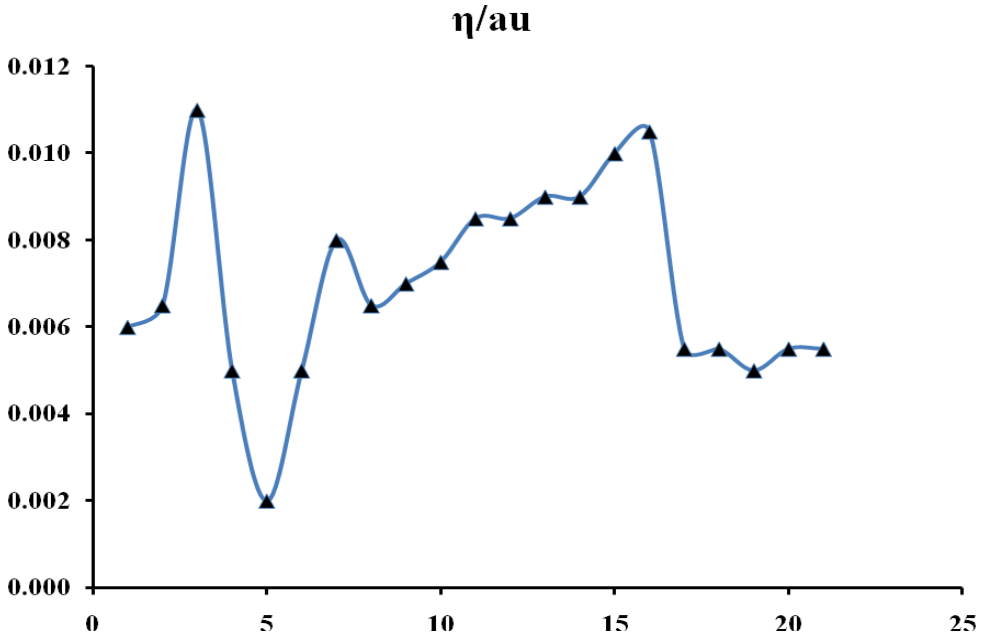

Figure 6.4 Variation of the chemical hardness (η) of all the complexes

The minimum electrophilicity principle (MEP) is formulated on the basis of MHP where there exits an inverse relationship between hardness (η) and chemical potential (μ). Lastly, we have used the MEP to explain the stability of the selected complexes. Figures 6.5 and 6.6 explain the variation of electrophilicity (ω) and chemical potential (μ), respectively. If we look at the values of electrophilicity (ω) and chemical potential (μ) we observed an inverse relationship between the two. The value of electrophilicity (ω) is found to be minimum for the complex 1 and it is maximum in case of complex 5.

Hence, form the study of the global reactivity descriptors we can conclude that compound 1 and 3 are the most stable complexes following the MEP and MHP, respectively and compound 5 is the most unstable species amongst all the complexes under study.

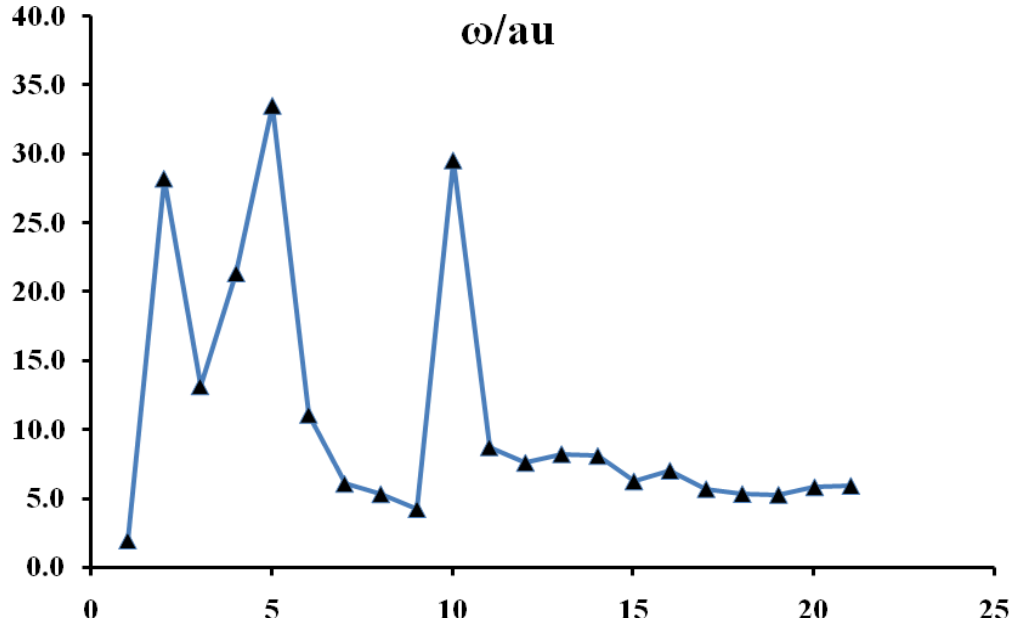

Figure 6.5 Variation of electrophilicity index (ω) of all the complexes

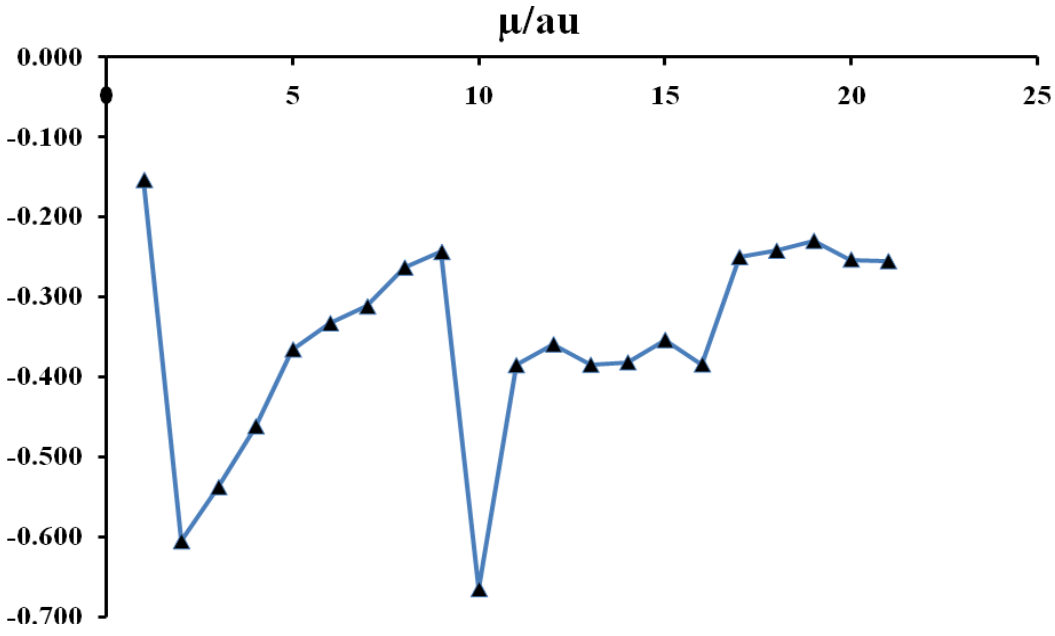

Figure 6.6 Variation of chemical potential (μ) of all the complexes

6.3.3 DFT based QSAR Models

Initially, we have performed simple linear regression for all the selected Au (III) complexes by considering the pIC_{50} as dependent variable and other descriptors as

single individual independent variable. However, the correlation of pIC_{50} with all the individual descriptors is found to be very much insignificant. Therefore, we have performed multiple regression analysis (MLR) to correlate the activity with the calculated DFT based descriptors.

In MLR analysis, we have used various combinations of the calculated descriptors in order to generate efficient regression models. The predictability of the models is determined using the "leave one out (LOO)" cross-validation method.[44,45] This method has been suggested by Dietrich et al.[46] and Cornish-Bowden and Wang[47], in which a compound is considered to be an outlier if its corresponding jackknife (R_j^2) value is higher than the other jackknife values. We have employed this method to increase the overall quality of our developed model. The jackknife values for the complexes are also tabulated in Table 6.1. It has been observed from Table 6.1 that compound 5, 6, 14, 17, 19 and 20 have exhibited higher values of R_j^2 (0.783, 0.764, 0.740, 0.778, 0.771 and 0.748, respectively) and thus we have eliminated these compounds to increase the overall quality of our developed models. Ultimately, we are leaving with fifteen molecules and these molecules are being used to generate the QSAR models.

The QSAR models with the absolute values of the statistical parameters are presented in Table 6.2. The values computed by considering the pIC_{50} as dependent variables against the selected parameters that has been evaluated. The descriptors that have been used in the development of the models are fully independent with each other or they have the least correlation. The autocorrelation values of the descriptors are also include in the Table 6.2. Form the result, it has been found that our developed models are very much effective in describing the cytotoxicity of the complexes under study, having R^2 in the range of 0.809-0.910.

Table 6.2 QSAR models with the statistical parameters for the selected Au (III) complexes

No	QSAR Models	N	R^2	SE	F	Auto correlation
E_1	-32.87(±11.52) -1998.61(±836.50) E_{L-H} -230.81(±30.80) E_{HOMO}	15	0.830	1.120	29.308	0.124
E_2	-32.87 (±11.52) -3997.21(±1673.02) η-230.81(±30.80) E_{HOMO}	15	0.830	1.120	29.308	0.119
E_3	-40.83(±10.71) -0.13 (±0.07) MR -204.50(±28.80)E_{HOMO}	15	0.809	1.794	25.385	0.012
E_4	-32.87(±11.52) -3535.58(±1643.07) η -230.81(±30.80) E_{LUMO}	15	0.830	1.120	29.308	0.099
E5	-32.87(±11.52) -1767.79(±821.54) E_{L-H}-230.81(±30.80) E_{LUMO}	15	0.830	1.120	29.308	0.103
E_6	-40.18(±10.52) -0.11(±0.07) MR -207.59 (±28.91) E_{LUMO}	15	0.812	1.687	25.967	0.006
E_7	-21.98 (±7.20) +3.69 (±0.57) ω -24.57 (±34.04) E_{NL}	15	0.895	0.730	51.292	0.354
E_8	-45.30(±11.61) -1647.2(±775.20)E_{L-H}-236.17(±29.79) $E_{(HOMO-1)}$	15	0.845	0.910	32.784	0.115
E_9	-45.30(±11.61) -3294.41(±1550.42) η -236.17(±29.79) $E_{(HOMO-1)}$	15	0.845	0.910	32.784	0.111
E_{10}	-51.18(±11.11) -0.11(±0.06) MR -214.48(±28.17) $E_{(HOMO-1)}$	15	0.830	1.138	29.191	0.008
E_{11}	-32.87(±11.52) -230.81 (±30.80) μ-1883.19(±828.91) E_{L-H}	15	0.830	1.120	29.308	0.113
E_{12}	-31.31 (±8.01) +3.97(±0.35) ω+966.82 (±509.70) E_{L-H}	15	0.916	0.321	65.373	0.087
E_{13}	-14.55 (±5.57) -0.40 (±0.54) logP+3.84(±0.44)ω	15	0.896	0.719	51.428	0.087
E_{14}	-40.51(±10.62) -0.12 (±0.07) MR-206.05 (±28.86)μ	15	0.811	11.740	25.677	0.008
E_{15}	-25.70 (±6.13)+ 0.07(±0.05) MR+4.13(±0.38)ω	15	0.910	0.578	60.907	0.077
E_{16}	-13.57(±9.30) -0.056 (±0.12) Pol+3.88(±0.46) ω	15	0.893	0.835	49.931	0.208

Furthermore, in order to ascertain the relative importance of the descriptors involved in the QSAR models, the P-values using F-statics are computed. These values characterize the importance of the independent variables in multiple regression. The descriptor in any model is significant only if its corresponding P-value is <0.05. The P-values for each variable in the regression model are shown in Table 6.3. It can be interpreted form this table that it is the E_{HOMO}, E_{LUMO}, $E_{(HOMO-1)}$, electrophilicity (ω) and chemical potential (μ) which are the most influencing descriptors affecting the activity of this class of biologically active systems.

Table 6.3 Computed P-values using F-statics for all the models

Equations	**X1**	**X2**	**X1**	**X2**	**Dominating descriptor**
1	E_{L-H}		0.03418	7.30×10^{-6}	
2	η	E_{HOMO}	0.03418	7.30×10^{-6}	E_{HOMO}
3	MR		0.07702	1.25×10^{-5}	
4	η		0.05247	7.30×10^{-6}	
5	E_{L-H}	E_{LUMO}	0.05247	7.30×10^{-6}	E_{LUMO}
6	MR		0.10593	1.12×10^{-5}	
7	E_{NL}	ω	0.48433	3.26×10^{-5}	ω
8	E_{L-H}		0.05506	4.12×10^{-6}	
9	η	$E_{(HOMO-1)}$	0.05506	4.12×10^{-6}	$E_{(HOMO-1)}$
10	MR		0.10967	6.22×10^{-6}	
11	E_{L-H}	μ	0.04229	7.30×10^{-6}	μ
12	E_{L-H}	ω	0.08217	1.02×10^{-6}	ω
13	logP		0.47237	1.67×10^{-6}	
14	MR	μ	0.09015	1.18×10^{-5}	μ
15	MR	ω	0.13136	1.27×10^{-7}	ω
16	Pol		0.64495	2.37×10^{-6}	

The correlation plot between experimental and calculated pIC_{50} for the best fit model (Eqn. E_{12}) is shown in Figure 6.7. The derived QSAR model aided by regression analysis demonstrated that the inhibitory activity is highly correlated with the DFT-based descriptors, lowest unoccupied molecular orbital (E_{LUMO}), highest occupied molecular orbital (E_{HOMO}), electrophilicity (ω), chemical potential (μ) and $E_{(HOMO-1)}$.

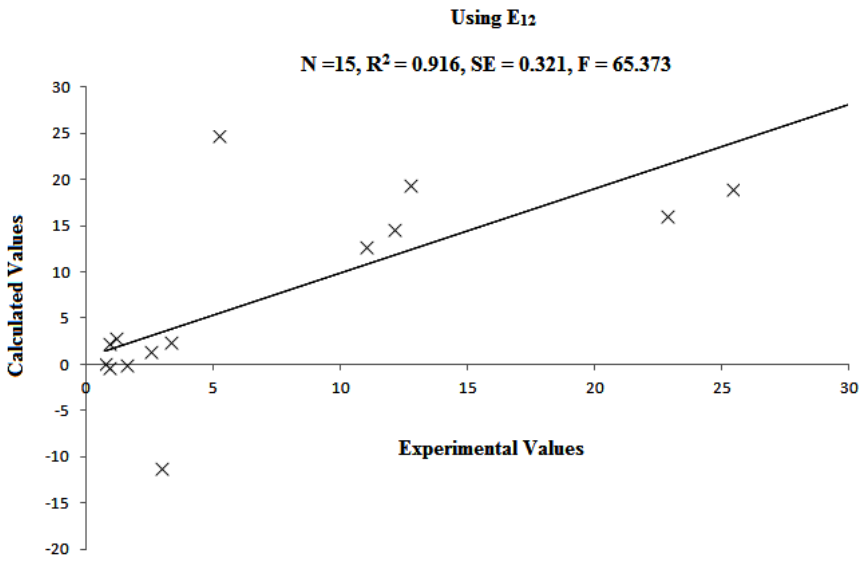

Figure 6.7 Best fit model amongst the derived equations

6.3.4 Docking Simulation

The crystallographic structure of the target protein *h*TrxR (PDB ID: 3QFA)[48] have been retrieved from the Protein Data Bank[49] at 2.20 Å resolution. The target *h*TrxR has four protein sequences, showing in different colours in Figure 6.8. Thioredoxin reductase is a homodimeric flavoprotein, therefore we have chosen only one chain to carry out our docking simulation. We have also eliminated water molecules to reduce the computational expenses. The optimized geometries (BLYP/DNP level of theory) of the Au (III) complexes have been utilized for the docking calculations. We have done our calculation using MVD in which flexible docking approach is used.

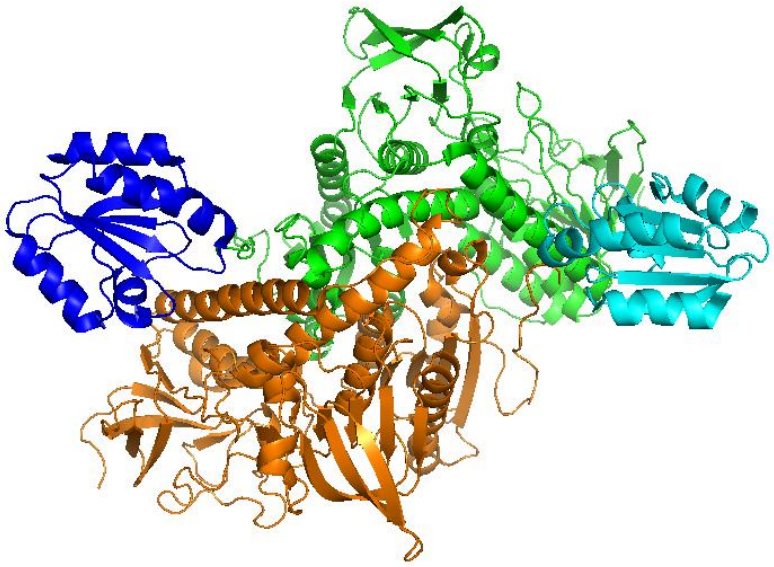

Figure 6.8 Protein sequences in *h*TrxR (PDB ID: 3QFA)

We have docked twenty one optimized Au (III) complexes, for fifty runs and 2000 interactions each, onto the active site of the protein *h*TrxR. Out of the twenty one compounds, only top five compounds have been considered based on Rerank score. The score of the different compounds with respect to the receptor for the top five molecules are presented in the Table 6.4. From Table 6.4, it has been found that compound 18 is having the best score amongst all the compounds that has been considered for our calculations. The binding poses of top five compounds with respect to the binding cavity are shown in Figures 6.9, 6.10, 6.11, 6.12 and 6.13. From Figure 6.9, it has been found that compound 18 fits well into the binding cavity of the *h*TrxR (best docked molecule). The amino acid residues which interact with compound 18 are Arg 226, Thr 58, Arg 166, Glu 163, Glu 341, Tyr 200, Phe 228, Val 340, Arg 293, Val 370, Thr 372, Gly 227. Thus, from the molecular docking study we can conclude that the some selected gold complexes are effective inhibitor of the target *h*TrxR. However, compound 18 is found to be the best inhibitor amongst all the studied complexes and it can induce mitochondrial inhibition by targeting the protein *h*TrxR.

Table 6.4 Docking score using Molegro Visual Docker (best five compounds)

Ligand	Mol Dock Score	Rerank Score	H-Bond
Compound 18	-176.182	-114.6	-0.29746
Compound 16	-164.891	-107.74	-1.95443
Compound 17	-168.244	-107.466	-1.90125
Compound 18 *(with different orientation)*	-175.976	-104.308	-4.76491
Compound 16 *(with different orientation)*	-178.825	-96.9964	-5.35626

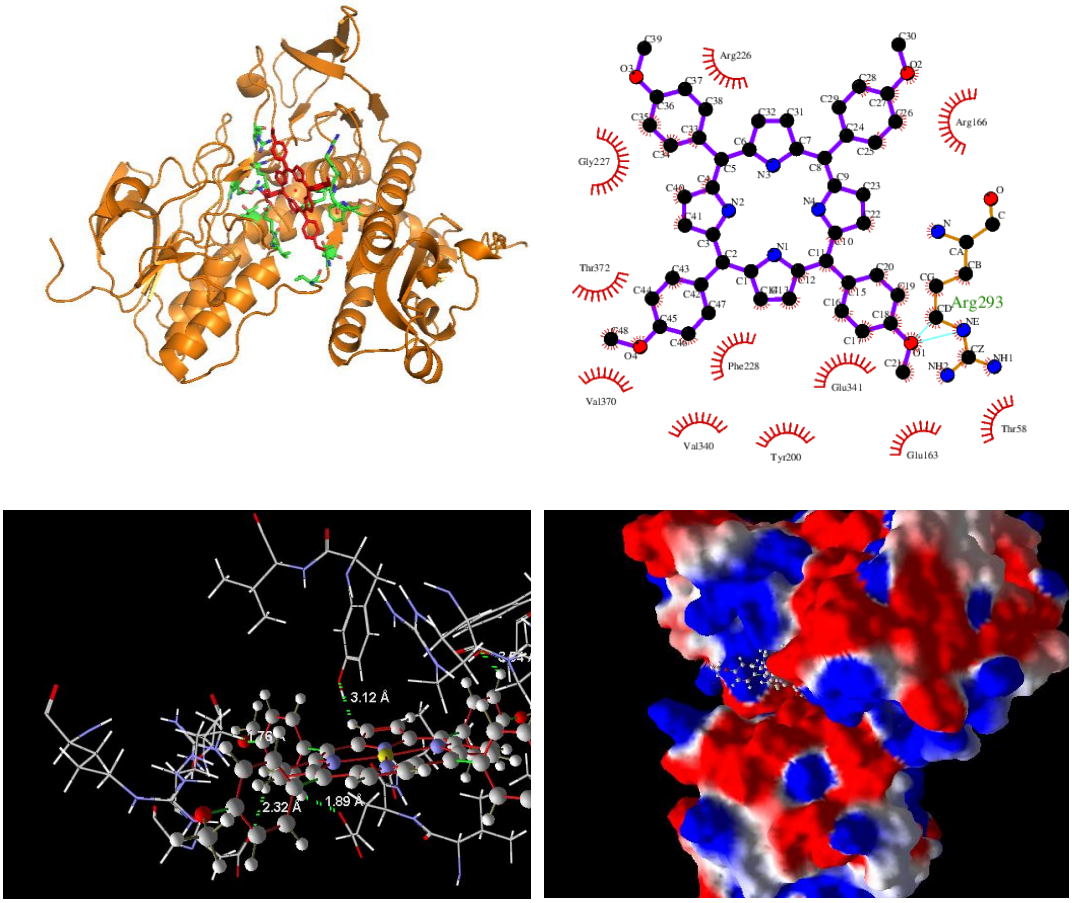

Figure 6.9 Docking pose of compound 18 at its highly bound cavity

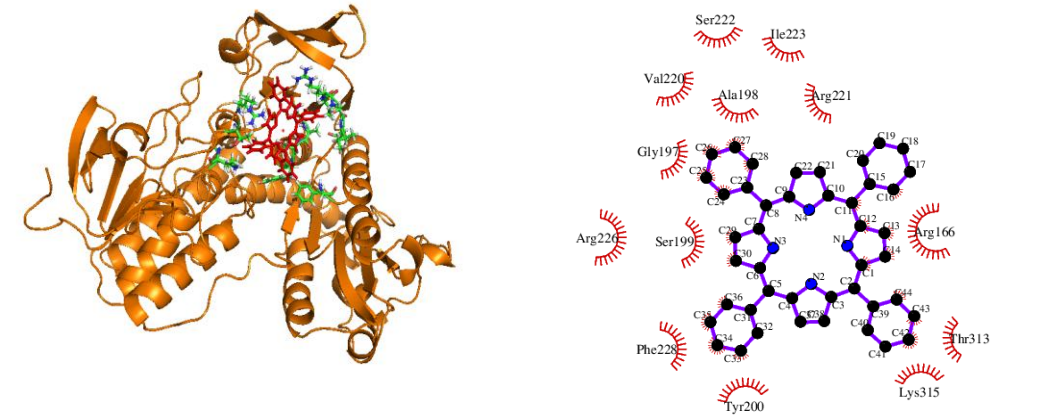

Figure 6.10 Docking pose of compound 16 at its highly bound cavity

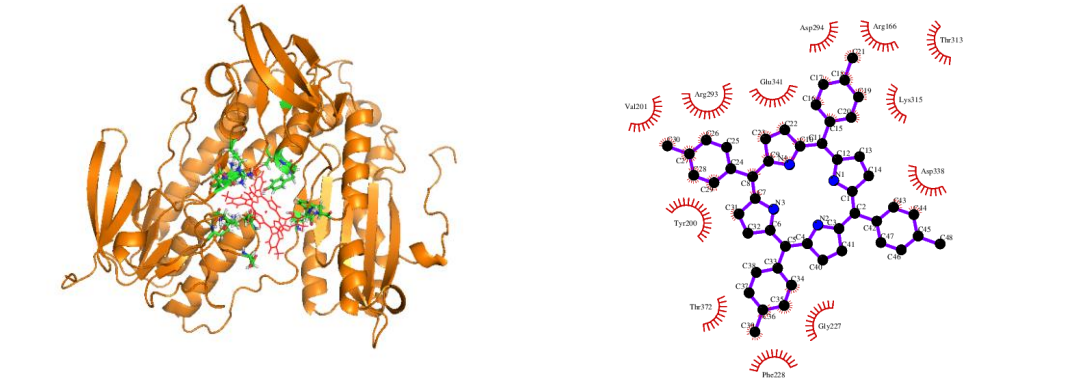

Figure 6.11 Docking pose of compound 17 at its highly bound cavity

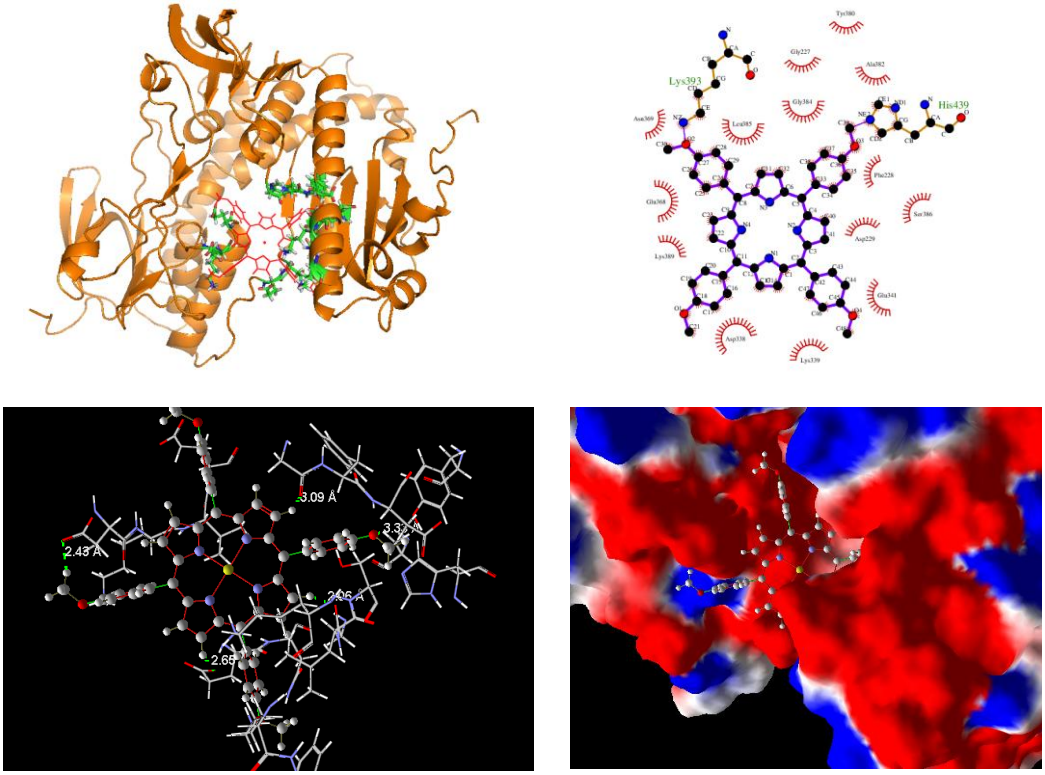

Figure 6.12 Docking pose of compound 18 at its highly bound cavity (with different orientation)

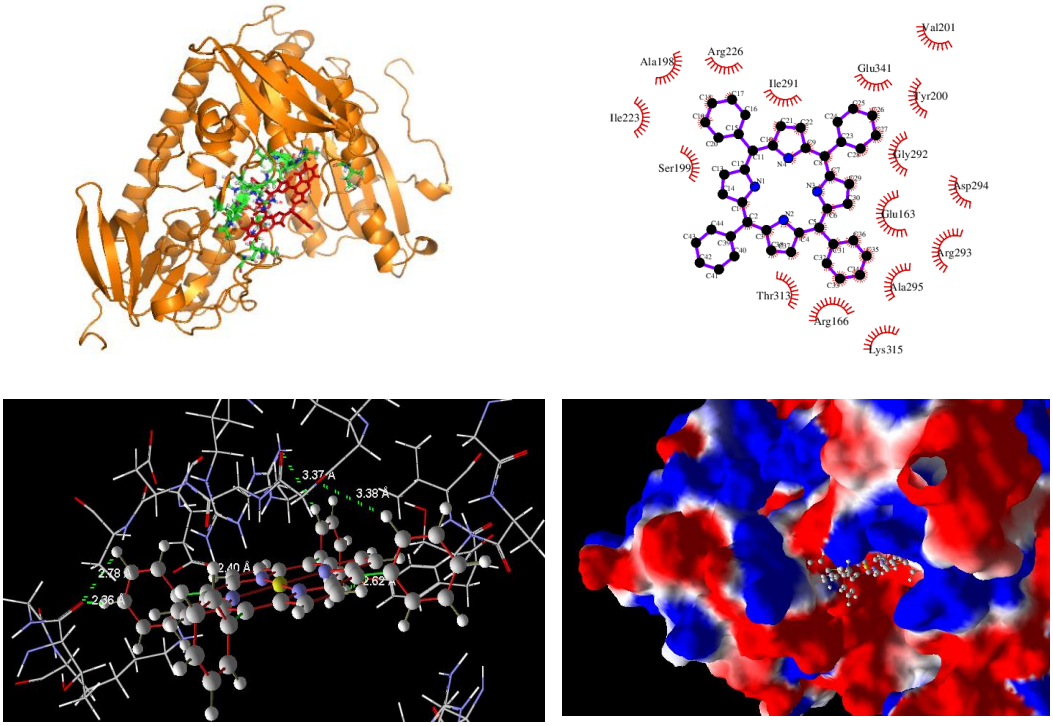

Figure 6.13 Docking pose of compound 16 at its highly bound cavity (with different orientation)

6.3.5 ADME Toxicity Study

6.3.5.1 Absorption

The absorption property of the molecules are studied by three different parameters *i.e*. Caco-2 permeability, human intestinal absorption (HIA) and *p*-glycoprotein (*P*-gp) substrate and inhibitor.

Caco-2 is the human epithelial colon cancer cells and these cells are used for the study of intestinal absorption in terms of permeability co-efficient of a drug and other molecules. It possesses multiple drug transport pathways through the intestinal epithelium. Higher Caco-2 cell permeability predicts good human oral bioavailability.[50] From the pkCSM data, presented in Table 6.5, it has been found that all the molecules have good permeability through Caco-2 intestinal surface except compound 1 and 6, having values less than 1.0. Since, Caco-2 cell line lacks CYP1A4 expression, it is insufficient to give the actual picture of the intestinal absorption of a molecule.[51] So, human intestinal absorption (HIA) study was carried out separately, which are shown in Table 6.5. HIA of a drug is a measure of bioavailability and absorption profile evaluated from the ratio of solubility and stability in the gastrointestinal tract, absorption through the intestinal wall, and a low rate of first-pass hepatic metabolism. Moreover, it is also dependent on the active transport mechanisms, passive membrane penetration, solubility of the drug, metabolism in the gastrointestinal tract, solubility and dissociation rate of the drug.[52] From Table 6.5, it has been observed that except compound 8 all the compounds are found to be permeable through human intestinal membrane.

To make the drug permeable to intestine and Blood Brain (BB) barried, *p*-glycoprotein (*P*-gp) plays an important role. *P*-gp is an efflux transporter that distributed in various organs like intestine, brain, kidney etc. It is also known as multidrug resistance protein-1 as its overexpression inhibits the activity of antitumor drugs. So, the better efficacy of a drug molecule, *P*-gp activity should not be overexpressed.[53] From the results of pkCSM, it is clear that all the compounds have *P*-gp substrate activity (Table 6.5). On the other hand eight compounds *viz.* compound 1, 2, 3, 4, 5, 6, 7 and 10 and nine compounds (1, 2, 3, 4, 5, 6, 7, 8 and 10) showed no inhibitory activity against *P*-gp-I and *P*-gp-II, respectively. This result implies a total number of eleven compounds starting from compound 11 to 21 may have some

adverse effect on *P*-gp activity and they might cross the membrane barrier without accumulation in the plasma.

Table 6.5 Absorption profile of the gold compounds

	Absorption				
No	**Caco-2 permeability log Papp in 10^{-6} cm/s**	**HIA % absorbed**	***P*-gp substrate**	***P*-gp-I inhibitor**	***P*-gp-II inhibitor**
1	0.171	80.05	Yes	No	No
2	1.188	100	Yes	No	No
3	1.158	98.429	Yes	No	No
4	1.22	97.616	Yes	No	No
5	1.309	98.143	Yes	No	No
6	0.258	100	Yes	No	No
7	1.238	100	Yes	No	No
8	1.363	1.363	Yes	Yes	No
9	1.252	95.248	Yes	Yes	Yes
10	1.33	100	Yes	No	No
11	1.117	97.983	Yes	Yes	Yes
12	1.313	93.765	Yes	Yes	Yes
13	1.113	97.205	Yes	Yes	Yes
14	1.116	96.367	Yes	Yes	Yes
15	1.18	96.336	Yes	Yes	Yes
16	1.109	96.428	Yes	Yes	Yes
17	1.277	100	Yes	Yes	Yes
18	1.271	100	Yes	Yes	Yes
19	1.191	100	Yes	Yes	Yes
20	1.253	99.951	Yes	Yes	Yes
21	1.262	100	Yes	Yes	Yes

6.3.5.2 Distribution and Metabolism

Blood Brain (BB) barrier is structural and chemical barrier between brain and systemic circulation to protect brain tissue from invasion by foreign harmful substances. It also helps in regulating the transport of some essential molecules and provides a stable environment. The BB barrier values for all the molecules are provided in Table 6.6. From the table, it has been observed that only two compounds *i.e.* 14 and 16 exhibit good affinity to cross the BB barrier with values more than 1.0. The other compounds exhibit relatively lower BB barrier penetration values compared to these two compounds. In our study, central nervous system (CNS) permeability, presented in Table 6.6, is also investigated and found that none of the compound exhibits permeability property to cross the CNS.

In human, cytochrome P450, a ubiquitous superfamily of enzyme also plays an important role in drug metabolism. Among all these, cytochrome P450 (CYP) families CYP450-1, CYP450-2 and CYP450-3 are more responsible for this function as they have broad substrate range. These enzymes can be induced and inhibited by certain drugs and other dietary compounds which may result into some clinically significant drug-drug interaction that can cause therapeutic failure or other adverse effects.[54-55] So, in our study we tested the substrate and inhibitors of some of these cytochrome P450 enzymes and the result we obtained is listed in the Table 6.6. From this analysis it was found that among all the molecules, sixteen compounds (1-16) are not showing the substrate property for CYP2D6 whereas all the compounds do not posses any inhibitory activity against this enzyme. Similarly, six compounds *viz.* compound 1, 2, 3, 5, 6 and 7 are not the substrate for CYP3A4 whereas only compound 19 has the inhibitory property against this enzyme. The inhibitory property of the compounds against CYP3A2, CYP2C19, CYP2C9 and CYP3A4 are also analysed and found that compound 4, 5, 8 and 9 can inhibit CYP3A2 activity, whereas, compound 5 and 19 can inhibit CYP2C19 and compound 19 posses dual inhibiting properties against CYP2C9 and CYP3A4 enzymes.

Table 6.6 Distribution and metabolism profile of the gold compounds

No	Distribution		Metabolism						
	BBB Permeability log BB	**CNS Permeability log PS**	**CYP2D6 Substrate**	**CYP3A4 Substrate**	**CYP1A2 Inhibitor**	**CYP2C19 Inhibitor**	**CYP2C9 Inhibitor**	**CYP2D6 Inhibitor**	**CYP3A4 Inhibitor**
1	-0.276	-4.024	No	No	No	No	No	No	No
2	-0.178	-2.918	No	No	No	No	No	No	No
3	-0.041	-3.752	No	No	No	No	No	No	No
4	0.726	-3.412	No	Yes	Yes	No	No	No	No
5	0.636	-0.893	No	No	Yes	Yes	No	No	No
6	-0.845	-3.463	No	No	No	No	No	No	No
7	-0.125	-3.377	No	No	No	No	No	No	No
8	0.329	-2.424	No	Yes	Yes	No	No	No	No
9	0.497	-1.342	No	Yes	No	No	No	No	No
10	0.038	-2.37	No	Yes	Yes	No	No	No	No
11	0.769	-4.093	No	Yes	No	No	No	No	No

12	0.509	-1.545	No	Yes	No	No	No	No	No
13	0.909	-4.184	No	Yes	No	No	No	No	No
14	1.105	-4.035	No	Yes	No	No	No	No	No
15	0.272	-1.433	No	Yes	No	No	No	No	No
16	1.049	-4.276	No	Yes	No	No	No	No	No
17	0.893	-0.35	Yes	Yes	No	No	No	No	No
18	0.856	-0.295	Yes	Yes	No	No	No	No	No
19	0.113	-1.463	Yes	Yes	No	Yes	Yes	No	Yes
20	0.59	-0.295	Yes	Yes	No	No	No	No	No
21	0.658	-0.295	Yes	Yes	No	No	No	No	No

6.3.5.3 Excretion and Toxicity

Total clearance of the drug (log ml/min/kg) and substrate specificity for renal OCT2 is assessed using pKCSM tool to check the excretion of the unused drug form the body. The results are shown in Table 6.7.

Table 6.7 Excretion and Toxicity profile of the gold compounds

No	Excretion		Toxicity		
	Renal OCT2 Substrate	**Total Clearance log ml/min/kg**	**AMES toxicity**	**Oral Rat Acute Toxicity (LD_{50}) mol/kg**	**Hepatotoxicity**
1	No	0.406	No	1.755	No
2	No	0.133	No	2.909	No
3	No	-1.065	No	2.076	No
4	No	-0.081	No	3.376	No
5	No	-0.058	Yes	2.375	No
6	No	-0.575	Yes	2.515	No
7	No	1.543	No	2.794	Yes
8	No	1.811	No	2.749	No
9	No	0.906	No	2.925	No
10	No	1.886	No	2.514	Yes
11	No	1.785	No	3.413	No
12	No	-0.794	No	2.51	No
13	No	1.912	No	3.412	No
14	No	0.802	No	3.401	No
15	No	-0.531	No	2.993	No
16	No	0.692	No	3.4	No
17	No	3.055	No	2.887	No
18	No	3.285	No	2.855	No
19	No	3.454	No	2.721	No
20	No	-1.084	No	2.755	No
21	No	-0.981	No	2.792	No

Form the data obtained, it is clearly demonstrated that none of the compounds showed substrate property for renal OCT2. Furthermore, the results give the amount of unused drugs which is than further excreted by the body.

To check the excretion of the unused drugs from the body, we investigated total clearance of the drug (log ml/min/kg) and also checked the substrate property for renal OCT2 using pkCSM tool, shown in Table 6.7. The result gives the amount of the unused drugs which is then further execrated by the body and it has also been found that none of the compounds are showing substrate property for renal OCT2.

In silico ames toxicity is performed to check the carcinogenicity of the compounds along with the determination of LD_{50} values for oral rat acute toxicity using the same tool. It is an initial screening process for a molecule to be considered as a drug. From the results of Table 6.7, it was found that none of the compound, except 5 and 6, show carcinogenic effect in AMES toxicity study. The determined LD_{50} values for oral rat acute toxicity also listed in the Table 6.7.

6.4 Conclusion

In this chapter, we have combine different computational techniques to screen some selected anticancer Au (III) candidates. DFT study reveals that compound 1 and 3 are most stable based on the MEP and MHP and compound 5 is the most unstable one. We have also build some DFT based effective regression models in order to correlate with the cytotoxictiy of the selected compounds. These regression models reveal that DFT based descriptors such as lowest unoccupied molecular orbital (E_{LUMO}), highest occupied molecular orbital (E_{HOMO}), electrophilicity (ω), chemical potential (μ) and $E_{(HOMO-1)}$ are powerful in describing the cytotoxicity.

Molecular docking study confirms that the selected gold complexes are effective inhibitor of the target protein *h*TrxR. However, compound 18 is found to be the best inhibitor amongst all the studied molecules. We have also performed ADME toxicity study in order to evaluate the pharmacokinetic properties of the complexes.

Based on regression, molecular docking and ADME toxicity studies, we can conclude that ethylenediamine, cyclam and meso-tetraarylporphyrins ligand containing compounds are the best molecules in terms of stability, safety and efficacy.

In summary, this work paves the way to explore different computational techniques to screen out potential drug candidates from the list of possible ones. Combine study of DFT along with molecular docking and ADME toxicity provide a better insight towards the discovery of novel chemical entity with relatively lesser side effects and efficacy. This initial work will eventually lead to the development of drug with higher success rates.

References

1. Tiekink, E.R. *Crit. Rev. Onc. Hematol.* **42** (3), 225--248, 2002.
2. Shaw, C.F. III *Chem. Rev.*, **99** (9), 2589--2600, 1999.
3. Messori, L., & Marcon, G. *Met. Ions. Biol. Syst.* **42,** 385--424**,** 2004.
4. Che, C.M., et al. *Chem. Commun.* **14,** 1718--1719, 2003.
5. Ronconi, L., et al. *Inorg. Chem.* **44** (6), 1867--1881, 2005.
6. Messori, L., et al. *J. Med. Chem.* **43** (19), 3541--3548, 2000.
7. Giovagnini, L., et al. *J. Med. Chem.* **48** (5), 1588--1595, 2005.
8. Buckley, R.G., et al. *J. Med. Chem.* **39** (26), 5208--5214, 1996..
9. Coronnello, M. et al. *J. Med. Chem.* **48** (21), 6761--6765, 2005.
10. Marcon, G., et al. *J. Med. Chem.* **45** (8), 1672--1677, 2002.
11. Messori, L., et al. Bioorg. Med. Chem. **12** (23), 6039--6043, 2004.
12. Rosenberg, B. *Cancer* **55** (10), 2303--2316, 1985.
13. Rosenberg, B., et al. *Nature* **222**, 385--386, 1969.
14. Tiekink, E. R. T. *Gold Bull.* **36** (4), 117--124, 2003.
15. Tiekink, E. R. T *Inflammopharmacology* **16**, 136--142, 2008.
16. Abbate, F., et al. *Inorg. Chim. Acta* **311** (1-2), 1--5, 2000.
17. Gabbiani, C., et al. *Gold Bull.* **40** (1), 73--81, 2007.
18. Messori, L., et al. *J. Med. Chem.* **43** (19), 3541--3548, 2000.
19. Rigobello, M.P., et al. *Br. J. Pharmacol.* **136** (8), 1162--1168, 2002.
20. Rigobello, M.P., et al. *J. Inorg. Biochem.* **98** (10), 1634--1641, 2004.
21. McKeagea, M.J., et al. *Coord. Chem. Rev.* **232** (1–2), 127--135, 2002.
22. Rigobello, M.P., et al. *Biochem. Pharmacol.* **67** (4) 689--696, 2004.
23. Bernardi, P. *Physiol. Rev.* **79**, 1127--1155, 1999.
24. Zoratti, M., & Szabo, I. *Biochim. Biophys. Acta* **1241** (2), 139--176, 1995.

25. McKeage, M.J., et al. *Coord. Chem. Rev.* **232** (1-2), 127--135, 2002.

26. Delly, B. *J. Chem. Phys.* **92**, 508--517, 1990.

27. Becke, A.D. *J. Chem. Phys.* **98**, 5648--5652, 1993.

28. Becke, A.D. *Phys. Rev. A.* **38** (6), 3098--3100, 1988.

29. Gordon, M.S. *Chem. Phys. Lett*. **76** (1), 163--168, 1980.

30. Heher, W.J., et al. *J. Chem. Phys.* **56**, 2257--2261, 1972.

31. HyperChemTM Release 2 for Windows, Autodesk Inc, 1992.

32. Singh, S.P., et al. *Med. Chem. Res.* **22** (10), 4755--4765, 2013.

33. Seal, A., et al. *Bioinformation* **5** (10), 430--439, 2011.

34. Bindoli, A., et al. *Coord. Chem. Rev.* **253** (11--12), 1692--1707, 2009.

35. Rajkhowa, S., et al. *J. Mol. Graphics Modell.* **62**, 56--68, 2015

36. Pires, D.E.V., et al. *J. Med. Chem.* **58** (9), 4066--4072, 2015.

37. Karelson, M. *Molecular descriptors in QSAR/QSPR*, Wiley-Interscience, New York, 2000.

38. Barua, N., et al. *Chem. Biol. Drug. Des.* 79, 553--559, 2012.

39. Thakur, A., et al. *Bioorg. Med. Chem.* 12(5), 1209--1214, 2004.

40. Jia, M., et al. *Int. J. Mol. Phys. B* **19**, 2939--2949, 2005.

41. Ghosh, D., & Jana, J. *Int. J. Quantum Chem.* **92**, 484--505, 2003.

42. Parr, R.G., & Chattaraj, P.K. *J. Am. Chem. Soc.* **113** (5), 1854--1855, 1991.

43. Morell, C., et al. *Phys. Chem. Chem. Phys.* **11** (18), 3417--3423, 2009.

44. Sarmah, P., & Deka, R.C. *J. Comput. Aided. Mol. Des.***23**, 343--354, 2009.

45. Barua, N., et al. *Chem. Biol. Drug. Des*. **79**, 553--559, 2012.

46. Dietrich, S.W., et al. *J. Med. Chem.* **23**, 1201--1205, 1980.

47. Cornish-Bowden, A., & Wong, J.T. *Biochem. J* **175**, 969--976, 1978.

48. Wolf, K.F., et al. *Nat. Commun.* **2**, 383--383, 2011.

49. Berman, H.M., et al. *Nucleic Acids Res.* **28** (1), 235--242, 2000.

50. Yazdanian, M., et al. *Pharm. Res.* **15** (9), 1490--1494, 1998.

51. van Breemen, R.B., & Li, Y. *Expert. Opin. Drug. Metab. Toxicol.* **1** (2), 175--85, 2005.

52. Wessel, M.D., et al. *J. Chem. Inf. Comput. Sci.* **38** (4), 726--735, 1998.

53.Horn, J.R. Drug Transporters: The Final Frontier for Drug Interactions. http://www.pharmacytimes.com/publications/issue/2008/2008-12/2008-12-8474, 2008.

54. Liu, J., et al. *Molecules* **18** (12), 14470--14495, 2013.

55. Lynch, T., & Price, A. *Am. Fam. Phys.* **76** (3), 391--396, 2007.